

Study of decoherence in radial local phonon hopping within trapped-ion string

Yu-Xuan Chen^{1,*}, Takumi Yuri¹, and Kenji Toyoda^{2,†}

¹*Graduate School of Engineering Science, Osaka University,
1-3 Machikaneyama, Toyonaka, Osaka 560-8531, Japan and*

²*Center for Quantum Information and Quantum Biology,
Osaka University, 1-2 Machikaneyama, Toyonaka, Osaka 560-0043, Japan*

(Dated: November 8, 2024)

We systematically investigate local phonon hopping in the radial direction of a linear trapped-ion string. We measure the decay of hopping as a function of key trap parameters and analyze the results in terms of the decay time and the number of oscillations. We attribute the loss of coherence to nonlinear coupling between different modes. Despite quantitative differences, the overall trends in our numerical simulations are similar to those of the experimental results. This work establishes a method for evaluating phonon hopping coherence and provides insight into the underlying decoherence mechanisms.

I. INTRODUCTION

A trapped-ion system is considered to be an excellent platform for quantum computing because of its exceptional performance in quantum information processing [1, 2]. It involves trapping ions using electromagnetic fields and applying laser pulses to precisely manipulate and measure quantum states [3, 4]. This system has a long coherence time, high-fidelity quantum logic gate operation, and a highly scalable architecture, offering significant advantages for quantum computing, quantum simulations, and quantum sensing [5–8].

In trapped-ion systems, phonons can be used as a medium for transferring information between ions, whose internal states serve as qubits or pseudospins. By being associated with collective modes of motion, phonons enable the coupling and entanglement of quantum states through Coulomb interactions between ions and have a large information capacity due to the high dimensionality of their Hilbert space. Accurate manipulation of phonons is crucial for achieving precise and fast quantum computations, especially for realizing multi-ion quantum state entanglement and quantum gate operations. In addition, phonons can be used to simulate physical models that involve bosonic particles, such as the Bose-Hubbard model [9, 10], the spin-boson model [11], and the Holstein model [12, 13]. The vibrational modes in trapped ions and phonons have been demonstrated to be fundamental quantum computing building blocks [14–16].

Phonons in trapped ions can be categorized as either collective-mode phonons or local phonons. For collective-mode phonons, ions collectively oscillate due to strong Coulomb interactions [17, 18]. For local phonons, ions oscillate in modes that are approximately independent of each other because the confinement force acting on each ion in one direction is much stronger than the Coulomb forces. The ions can still be weakly coupled together by Coulomb interactions.

Studies of local phonons in trapped ions can be divided into those of phonons in multi-well potentials or trap arrays and those of phonons in the radial direction of a linear ion string. For the former type of phonon, each site can be controlled independently. Coupled quantized mechanical oscillators and the exchange (hopping) of local phonons between them have been examined using two ions in double-well potentials [19, 20]. Multiple potential wells, each containing a single ion, have been controlled to demonstrate the tunable coupling of phonons [21], their coherent coupling [22], and two-dimensional networks of vibrational modes [23, 24]. Regarding the latter type of phonon, Porras and Cirac proposed using local phonons in the radial direction of a linear ion string for simulating the Bose-Hubbard model [25]. The hopping of radial local phonons and their interference have been investigated [26–29]. Radial local phonons have been used to simulate the Jaynes-Cummings-Hubbard model and the Rabi-Hubbard model [30–33].

A system of local phonons in the radial direction of a linear ion string can be prepared in a standard linear trap and applied to quantum simulations or analog quantum computation [34]. Despite the importance of radial local phonons, some of their basic characteristics that may affect experimental implementations are not fully understood. One of the most important of these characteristics is the coherence in the phonon hopping process. The hopping of phonons occurs as an elementary process that can be expressed using a hopping Hamiltonian [25], which is key to applications using radial phonons. The process and coherence may be affected by various factors, including the residual thermal distribution in the system. The conditions for a well-defined concept of radial phonons, especially their number preservation, necessitate that the confinement force be much stronger than Coulomb forces, as mentioned above. To satisfy this condition, the axial confinement should be kept weak so that the inter-ion distances become relatively large (in our typical conditions with $^{40}\text{Ca}^+$ ions, we use inter-ion distances of $\sim 20 \mu\text{m}$ for a radial trap frequency of $\sim 3 \text{ MHz}$). Due to the relatively weak confinement along the axial direction and the resulting lack of Lamb-Dicke confinement, it is

* u320161d@ecs.osaka-u.ac.jp

† kenji.toyoda.qiqb@osaka-u.ac.jp

not straightforward to apply sub-Doppler or ground-state cooling mechanisms such as sideband cooling. We can avoid the direct effect of the axial thermal distribution (e.g., the appearance of Doppler sidebands) by setting the direction of the excitation lasers for the manipulation and observation of radial phonons perpendicular to the trap axis. The indirect effects of the residual axial thermal distribution, especially those on the coherence of phonon hopping, have not been previously investigated.

In this study, we investigate the hopping process of radial local phonons in a trapped-ion system, focusing on the coherence preservation and decoherence mechanisms for phonons in localized regions. We analyze the phonon hopping decoherence in terms of the decay time and the number of oscillations, which provide insights for understanding hopping behavior and system fidelity in processes involving phonons. Regarding the decoherence mechanism, we assume that the Coulomb interaction between ions triggers a nonlinear coupling between different vibrational modes in the y and z directions, leading to the generation of a Kerr-type Hamiltonian [35, 36]. In numerical simulations, although we do not obtain a quantitative agreement with experimental results up to a small ratio, we confirm similar overall trends to those in the experimental results, which validates our theoretical model.

II. EXPERIMENTAL PROCEDURE

We confined two $^{40}\text{Ca}^+$ ions in a linear Paul trap, with radio-frequency (RF) and direct-current fields providing radial and axial confinement. RF signals were fed to the trap electrodes through a helical resonator with a resonance frequency of 23.5 MHz. Regulating the RF amplitudes of the radial electrode voltages allowed us to stabilize the radial trap frequencies (ω_x, ω_y) [37]. The confinement along the axial direction was relatively weak, resulting in large inter-ion distances and the formation of a linear ion chain in the axial direction. We decomposed the motion of the ions into three-dimensional vibrations in axial (z) and radial (x and y) directions. The Hamiltonian governing the radial direction (the y direction in this study) can be written as follows [25]:

$$H_y = \sum_{i=1,2} \frac{p_i^2}{2m} + \sum_{i=1,2} \frac{1}{2} m \omega_y^2 y_i^2 - \frac{e^2}{8\pi\epsilon_0} \frac{(y_1 - y_2)^2}{|z_1 - z_2|^3}, \quad (1)$$

where y_i and z_i represent the spatial coordinates of the i -th ion in the ion chain, p_i is the ion momentum, m is the ion mass, and ω_y is the trap frequency in the radial y direction. The first two terms in the Hamiltonian represent the kinetic energy and trap potential, respectively, and the last term represents the Coulomb interaction, which induces phonon hopping. Then, we converted the Hamiltonian in Eq. (1) to its second quantized form. It can be rewritten using local-phonon operators as follows

[25]:

$$H_y = \sum_{i=1,2} \hbar \left(\omega_y - \frac{\kappa}{2} \right) a_i^\dagger a_i + \frac{\hbar\kappa}{2} (a_1 a_2^\dagger + a_1^\dagger a_2), \quad (2)$$

where

$$\kappa = \frac{e^2}{4\pi\epsilon_0 m \omega_y^2 d_0^3} \quad (3)$$

is the phonon hopping rate between ions 1 and 2. a_i and a_i^\dagger are annihilation and creation operators for the local phonon modes along the y direction of the i -th ion, respectively. d_0 is the inter-ion distance. Phonon hopping can also be explained as the normal mode of radial vibrational motion. Our previous study describes the specific details [26].

Two laser beams with wavelengths of 423 and 375 nm, respectively, were utilized for optical ionization. A two-step laser cooling technique was used to cool the ions to near the vibrational ground state. This consisted of Doppler cooling using the 397-nm ($S_{1/2}-P_{1/2}$) and 866-nm ($D_{3/2}-P_{1/2}$) transitions and resolved sideband cooling using the 729-nm ($S_{1/2}-D_{5/2}$) and 854-nm ($D_{5/2}-P_{3/2}$) transitions. After the resolved sideband cooling, the average phonon numbers in the radial directions were $(\langle n_x \rangle, \langle n_y \rangle) \sim (0.30, 0.04)$. The output of the 729-nm laser was split into two beams, each of which illuminated one of the two ions. Each beam was controlled by a dedicated single-pass acousto-optic modulator. This system of single-pass acousto-optic modulators allowed us to maintain the intensity of the laser beams irradiating the ions and equalizing the Rabi frequencies between the ions. The maximum carrier Rabi frequency for the $S_{1/2}(m_J = -1/2)-D_{5/2}(m_J = -1/2)$ transition was ~ 800 kHz and the corresponding Rabi frequencies for the sideband transitions involving the vibrational ground state were ~ 35 kHz.

The specific steps for local phonon hopping are as follows (see Fig. 1 for the experimental time sequence).

1. Perform Doppler and sideband cooling to cool the ions to their vibrational ground state.
2. Apply blue-sideband and carrier π pulses to one of the two ions (referred to as ion 1) to prepare the initial phonon state $|1\rangle_1|0\rangle_2$. Immediately after, apply an 854-nm laser pulse nearly resonance with the $D_{5/2} - P_{3/2}$ transition to pump the residual population in $D_{5/2}$.
3. Turn off all the lasers and let the phonon undergo hopping between the ions due to Coulomb interactions.
4. Irradiate both ions with a red-sideband π pulse to map the vibrational states onto the internal states. Applying a red-sideband π pulse causes an ion with a phonon number of 1 to be transferred to the internal excited state. No transition occurs if the

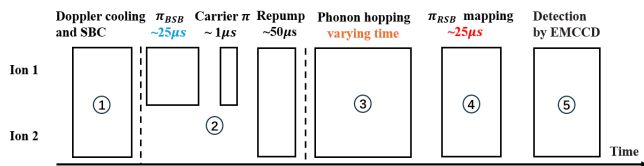


FIG. 1. Experimental time sequence for observing phonon hopping. SBC: sideband cooling; RSB/BSB: red/blue sideband; EMCCD: electron-multiplying charge-coupled device.

phonon number is 0 (i.e., the ground state is maintained). Determine the internal state using the shelving method.

5. Illuminate both ions with a 397-nm laser and use an electron-multiplying charge-coupled-device camera to image the fluorescence to detect the internal state of individual ions.

III. MEASUREMENT OF HOPPING DYNAMICS

According to Eq. (3), the local phonon hopping rate depends on d_0 , the inter-ion distance (which depends on the axial confinement), and ω_y , the trap frequency in the y direction. These parameters were varied in our systematic investigation of local phonon hopping decoherence.

In typical ion trap experiments, including the present experiment, the parameters given above are used to control the binding conditions of ions in the trap. As a result, they determine the configuration and motion of the ions. As discussed later, the factors that may affect the coherence of phonon hopping, such as nonlinear couplings between collective modes, may depend on factors such as the strength of inter-mode couplings and the velocity distribution in thermal states. These factors largely depend on the configuration and motion of ions and hence on the global trap parameters, as stated above. We thus chose the above parameters for the systematic investigation.

To quantify the coherence of hopping dynamics, we introduce the *number of oscillations*, defined as the number of cycles in the hopping process from the initial time until the contrast decreases to $1/e$ of its initial value.

A. Results for hopping dynamics

Figures 2 and 3 show data corresponding to the cases of the maximum number of oscillations and longest decay time in our experiment, respectively. The blue points represent the probability of being detected in an excited state, with each data point averaged over 20 measurements. The hopping frequency is determined by fitting a sinusoidal function. The obtained values are generally consistent with the theoretical prediction from Eq. (3).

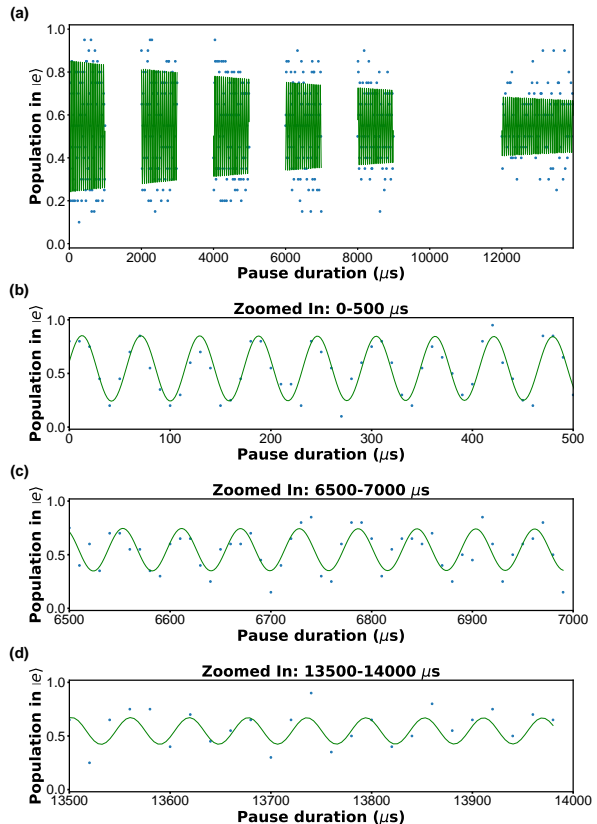


FIG. 2. Phonon hopping results corresponding to case of maximum number of oscillations in our experiment. The corresponding radial trap frequency $\omega_y/2\pi$ is 2.87 MHz and the inter-ion distance d_0 is 12.5 μm . The blue dots are the experimental measurements and the green curve is the result obtained from fitting the function $ae^{-bx} \sin(cx + d) + fx$. (a) Full experimental data and numerical calculations for phonon hopping. (b-d) Magnified views of different time periods for hopping process.

This analysis confirms the expected behavior of phonon hopping dynamics under various trap conditions, which is consistent with our theoretical model.

B. Systematic investigation of dependence on trap parameters

To investigate the dependence of the phonon hopping coherence on the radial trap frequency ω_y , we fixed the inter-ion distance d_0 at 16.4 μm and varied ω_y by adjusting the RF amplitude of the radial electrode voltages. The values of $\omega_y/2\pi$ examined here are {2.43, 2.64, 2.87, 3.11} MHz.

To investigate the dependence of the phonon hop-

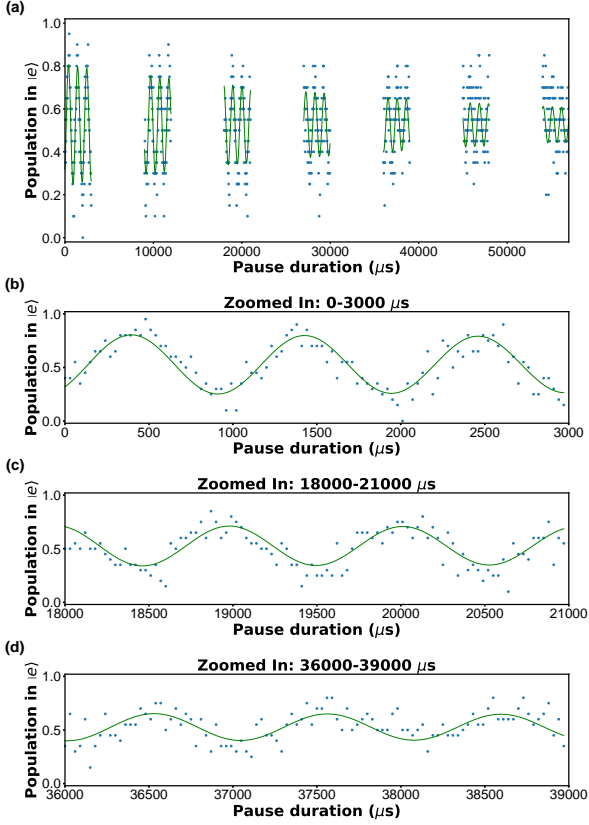


FIG. 3. Phonon hopping results corresponding to case of longest decay time in our experiment. The corresponding radial trap frequency $\omega_y/2\pi$ is 2.87 MHz and the inter-ion distance d_0 is $32.6 \mu\text{m}$. The blue dots are the experimental measurements and the green curve is the result obtained from fitting the function $ae^{-bx} \sin(cx + d) + fx$. (a) Full experimental data and numerical calculations for phonon hopping. (b-d) Magnified views of different time periods for hopping process.

ping coherence on d_0 , we controlled d_0 by varying the axial electrode voltage while maintaining a fixed value of 2.87 MHz for $\omega_y/2\pi$. The relation between d_0 and the axial trap frequency ω_z assumed here is $d_0 = (e^2/4\pi\epsilon_0 m\omega_z^2)^{1/3} (2.018/2^{0.559})$ [17]. The values of d_0 examined here are $\{12.5, 16.4, 20.1, 32.6\} \mu\text{m}$, which correspond to $\omega_z/2\pi$ values of $\{213, 140, 105, 50\}$ kHz, respectively.

The experimental results in Figs. 4 and 5 show the dependence of phonon hopping coherence on the inter-ion distance d_0 and the radial trap frequency ω_y . In Fig. 4 (Fig. 5), the two plots show the decay time (the number of oscillations) on the vertical axis. In both figures, the red circles with error bars are the results of the experi-

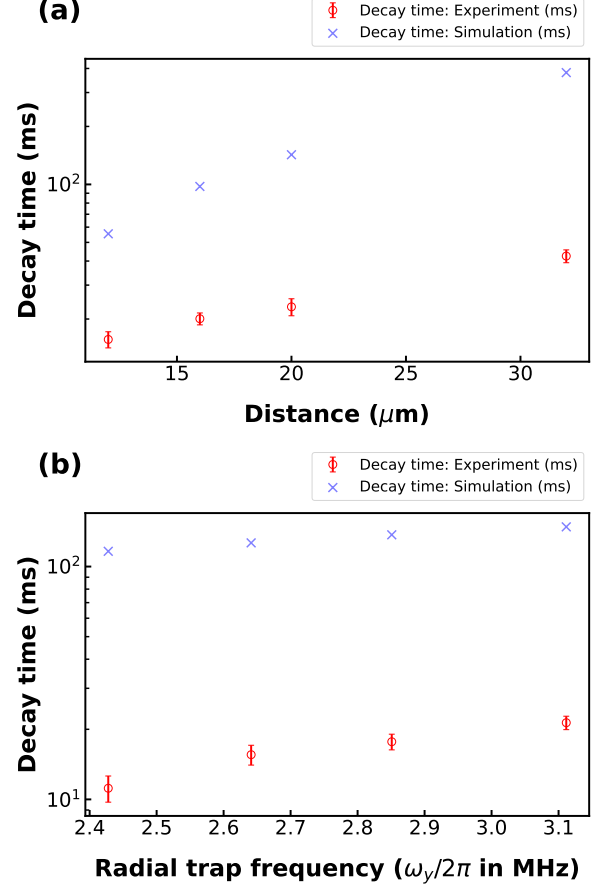


FIG. 4. Experimental results (indicated by red circles with error bars) and numerical simulations (indicated by blue crosses) showing dependence of decay time on inter-ion distance and radial trap frequency. (a) Decay time as function of inter-ion distance with data points at $d_0 = \{12.5, 16.4, 20.1, 32.6\} \mu\text{m}$. (b) Decay time as function of radial trap frequency with data points at $\omega_y/2\pi = \{2.43, 2.64, 2.87, 3.11\}$ MHz. The numerical simulations used the same parameter sets as those in the experiment.

ment and the blue crosses are the results of the numerical simulation.

As shown in Fig. 4(a), the decay time significantly increases with inter-ion distance, indicating that phonon coherence is better maintained at larger distances. Similarly, Fig. 4(b) shows that the decay time increases with increasing trap frequency. Fig. 5(a) shows that the number of oscillations decreases with increasing inter-ion distance. Conversely, Fig. 5(b) shows that the number of oscillations increases with increasing trap frequencies, which suggests enhanced coherence. In the next section, we introduce a model based on a nonlinear coupling between collective modes and interpret the global trends shown in Figs. 4 and 5.

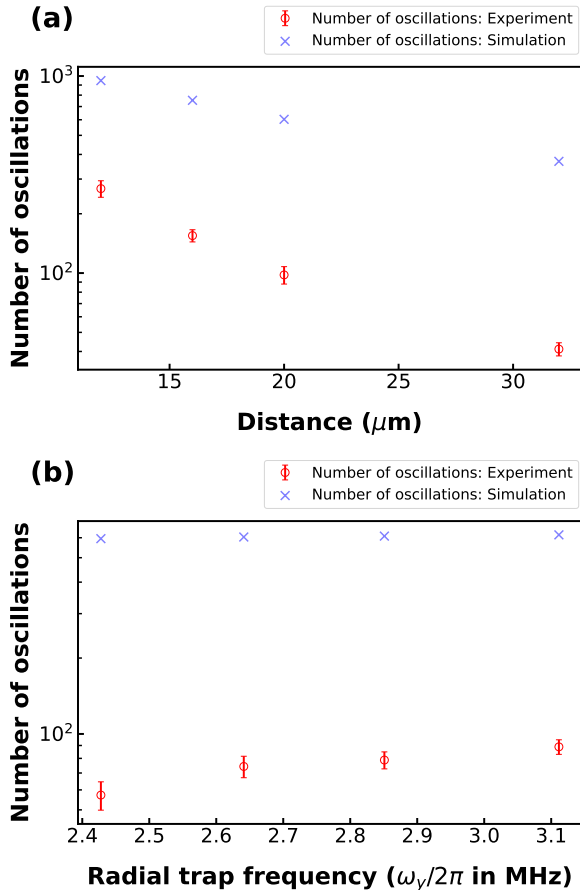


FIG. 5. Experimental results (indicated by red circles with error bars) and numerical simulations (indicated by blue crosses) showing dependence of number of oscillations on inter-ion distance and radial trap frequency. (a) Number of oscillations as function of inter-ion distance with data points at $d_0 = \{12.5, 16.4, 20.1, 32.6\}$ μm . (b) Number of oscillations as function of radial trap frequency with data points at $\omega_y/2\pi = \{2.43, 2.64, 2.87, 3.11\}$ MHz. The numerical simulations used the same parameter sets as those in the experiment.

IV. EFFECT OF INTER-MODE COUPLINGS DUE TO KERR NONLINEARITY ON PHONON HOPPING DECOHERENCE

In our experiment, the ions were cooled to the vibrational ground state in the x and y directions by sideband cooling. On the other hand, the condition of Lamb-Dicke confinement, which is almost a prerequisite for performing sideband cooling, was not satisfied in the z direction; only Doppler cooling was performed in this direction. For the values of axial trap frequency given above, the modified Lamb-Dicke parameter $\eta\sqrt{n_{\text{av}}}$, which accounts for finite temperature effects, ranges from 1.0 to 4.4. This indicates that the system was not fully within the Lamb-Dicke regime, as $\eta\sqrt{n_{\text{av}}} < 1$ was not satisfied for the

given range. In the case of two ions, the motion of the ions in the z direction can be decomposed into the center-of-mass and stretching modes. In the stretching mode, the ions oscillate with opposite phases, which leads to an inter-ion distance change. It is known that the stretching mode can be preferentially coupled to the rocking mode in the y direction, which also involves an inter-ion distance change via the nonlinearity in the Coulomb interactions [35, 36]. Here, we analyze the effect of this nonlinear coupling on the decoherence of phonon hopping.

A. Model of nonlinear coupling between radial and axial modes

The inter-ion distance d_0 influences the Coulomb interactions between ions. By varying d_0 , we modified the strength of these interactions, directly influencing vibrational mode coupling. A larger d_0 reduces the Coulomb interaction strength, leading to weaker mode coupling. This reduction in coupling lowers the nonlinear coefficients in the phonon-phonon coupling Hamiltonian, such as the Kerr-type Hamiltonian:

$$H_{\text{Kerr}} = \hbar\chi\hat{n}_r\hat{n}_s, \quad (4)$$

where \hat{n}_r and \hat{n}_s are the phonon number operators for the rocking mode in the y direction and the stretching mode in the z direction, respectively. The coupling constant χ is expressed as [36]:

$$\chi = -\omega_s \left(\frac{1}{2} + \frac{\omega_s^2/2}{4\omega_r^2 - \omega_s^2} \right) \left(\frac{\omega_z}{\omega_r} \right) \left(\frac{2\hbar\omega_z}{\alpha^2 mc^2} \right)^{1/3}, \quad (5)$$

where α denotes the fine-structure constant, c is the speed of light, and ω_s and ω_r are the stretching- and rocking-mode frequencies, respectively. Similarly, the radial trap frequency ω_y defines the ion confinement strength in the radial direction. By varying ω_y , we altered the vibrational states and energy levels, significantly impacting phonon dynamics.

The Hamiltonian for the Kerr-type coupling in Eq. (4) can be interpreted in the collective-mode Fock-state basis as a shift of the rocking mode frequency, which is proportional to the stretching-mode quantum number n_s , as follows:

$$\delta\omega_r = \chi n_s. \quad (6)$$

B. Principles of numerical simulation incorporating inter-mode couplings

To evaluate the magnitude of the shift of the rocking mode using Eqs. (5) and (6), we need the trap frequencies and the average vibrational quantum numbers along the axial direction. The axial trap frequency in various conditions can be evaluated with axial sideband spectroscopy

in combination with inter-ion distance measurements using fluorescence images. To evaluate the average vibrational quantum numbers along the axial direction, the heights of the axial sidebands can be used. They can be compared with a model for which a thermal quantum number distribution is assumed.

Since the axial motion was not in the Lamb-Dicke regime in our typical experimental conditions and we observed many sideband spectra, we did not fit model functions to each spectral component. Instead, we used a single Doppler-broadened envelope to fit the entire spectrum. We assumed that the axial motion is in thermal equilibrium with a temperature close to the Doppler limit $T_D = \hbar\Gamma/2k_B$. In the case of $^{40}\text{Ca}^+$ ions, the natural width of the $S_{1/2} - P_{1/2}$ transition is 20.4 MHz [38, 39]. The Doppler-limited temperature calculated on this basis is 490 μK . The Hamiltonian for the harmonic motion of the ions in the z direction can be described as follows:

$$H_z = \sum_{k=1,2} \left(\frac{p_{z,k}^2}{2m} + \frac{1}{2}m\omega_z^2 z_k^2 \right), \quad (7)$$

where $p_{z,k}$ is the momentum of the k -th ion along the z axis, z_k is the position coordinate of the k -th ion, m is the mass of the ion, and ω_z is the trap frequency in the z direction.

According to the equipartition theorem in thermodynamics [40], the average kinetic energy per degree of freedom at temperature T is $\frac{1}{2}k_B T$. We assumed that both ions are in thermal equilibrium. The sum of the average kinetic and potential energies is given by:

$$\sum_{k=1,2} \frac{p_{z,k}^2}{2m} = \sum_{k=1,2} \frac{1}{2}m\omega_z^2 z_k^2 = k_B T, \quad (8)$$

which can be simplified as:

$$\left\langle \frac{1}{2}mv_{z,1}^2 + \frac{1}{2}mv_{z,2}^2 \right\rangle = k_B T. \quad (9)$$

Assuming that the mean square velocities of both ions are equal, $\langle v_{z,1}^2 \rangle = \langle v_{z,2}^2 \rangle$, we obtain the following relation for the root mean square (rms) velocity $v_{\text{rms}} = \sqrt{\langle v_{z,i}^2 \rangle}$:

$$mv_{\text{rms}}^2 = k_B T. \quad (10)$$

From the equipartition theorem, we can also obtain the average total energy for the axial stretching mode. It can be represented as follows, considering that a harmonic oscillator mode has both kinetic and potential energies:

$$\hbar\omega_s \langle \hat{n}_s \rangle = k_B T, \quad (11)$$

where ω_s and $\langle \hat{n}_s \rangle$ are the oscillation frequency and the average quantum number for the axial stretching mode, respectively. From Eqs. (10) and (11), we can relate $\langle \hat{n}_s \rangle$ and v_{rms} as follows:

$$\langle \hat{n}_s \rangle = \frac{mv_{\text{rms}}^2}{\hbar\omega_s}. \quad (12)$$

The trap frequency and the average vibrational quantum number are obtained using the relation $d_0 = (e^2/4\pi\epsilon_0 m\omega_z^2)(2.018/2^{0.559})$ [17] and Eq. (7), respectively. The expression for calculating the hopping decoherence is as follows:

$$h(t) = \sum_{n=0}^N P_n \sin^2 \left[\frac{(\kappa - \chi^n)t}{2} \right], \quad (13)$$

where P_n is the phonon number distribution for the axial stretching mode, which is calculated by assuming a thermal distribution based on Eq. (12) with v_{rms} determined from experimental Doppler-broadened spectra. On this basis, the numerical simulation results for the decay time and the vibration frequency are compared with the experimental values (see Figs. 4 and 5).

C. Results of numerical simulation

In the numerical simulation, we chose sets of values for the inter-ion distance d_0 and the radial trap frequency ω_y that are similar to those used in the experiment and performed calculations. A comparison between the experimental data (indicated by red circles in Figs. 4 and 5) and the numerical simulation results (indicated by blue crosses in the same figures) shows consistent trends in the dependence of the decay time (Fig. 4) and the number of oscillations (Fig. 5) on the inter-ion distance and trap frequency. This supports our assumptions regarding the nonlinear coupling between the stretching mode and the rocking mode.

V. DISCUSSION

Studies of coherence in quantum systems often focus on the lifetime of superposition states. In contrast, we investigated phonon hopping coherence, which involves the coherence between different vibrational modes, such as the stretching and rocking modes. This mode-mode coherence indicates how well these modes remain phase-locked over time despite the nonlinear couplings induced by Coulomb interactions. The coherence observed in phonon hopping is critical for multi-mode quantum operations in ion trap systems, as it shows how these modes maintain phase coherence, which is vital for effective quantum information processing.

Despite the general agreement of the global trends, as presented in the previous section, there is a noticeable gap between the experimental and numerical simulation results in terms of the decay time and the number of oscillations. This discrepancy may arise from experimental conditions not perfectly replicating the harmonic potential, leading to enhanced nonlinear mode coupling. In experimental setups, imperfections in the trap potential can introduce anharmonic terms, increasing the likelihood of

higher-order mode couplings. The anharmonic potentials introduce additional terms in the system's Hamiltonian and the higher-order terms facilitate increased energy exchange between modes, causing additional decoherence not accounted for in the idealized simulation model.

VI. CONCLUSION

Our systematic experimental study demonstrates how the inter-ion distance and the radial trap frequency significantly affect phonon hopping coherence in trapped-ion systems. Our results show that increased inter-ion distances and radial trap frequencies enhance coherence by reducing nonlinear coupling effects. Numerical simu-

lations validated our assumption that the nonlinear coupling between different modes contributes to decoherence. Controlling mode-mode couplings is essential for advancing quantum information processing, as these interactions are critical for maintaining coherence in multi-mode quantum systems.

ACKNOWLEDGMENTS

This work was supported by the Ministry of Education, Culture, Sports, Science and Technology (MEXT) Quantum Leap Flagship Program (MEXT Q-LEAP) (grant number JPMXS0118067477) and the Japan Science and Technology Agency Moonshot Research and Development program (grant number JPMJMS2063).

-
- [1] J. I. Cirac and P. Zoller, Quantum computations with cold trapped ions, *Phys. Rev. Lett.* **74**, 4091 (1995).
 - [2] R. Blatt and D. Wineland, Entangled states of trapped atomic ions, *Nature (London)* **453**, 1008 (2008).
 - [3] D. Leibfried, R. Blatt, C. Monroe, and D. Wineland, Quantum dynamics of single trapped ions, *Rev. Mod. Phys.* **75**, 281 (2003).
 - [4] H. Häffner, C. F. Roos, and R. Blatt, Quantum computing with trapped ions, *Phys. Rep.* **469**, 155 (2008).
 - [5] C. Monroe and J. Kim, Scaling the ion trap quantum processor, *Science* **339**, 1164 (2013).
 - [6] K. R. Brown, J. Kim, and C. Monroe, Co-designing a scalable quantum computer with trapped atomic ions, *npj Quantum Inf.* **2**, 1 (2016).
 - [7] D. Porras and J. I. Cirac, Effective quantum spin systems with trapped ions, *Phys. Rev. Lett.* **92**, 207901 (2004).
 - [8] F. Schmidt-Kaler, H. Häffner, M. Riebe, S. Gulde, G. P. T. Lancaster, T. Deuschle, C. Becher, C. F. Roos, J. Eschner, and R. Blatt, Realization of the Cirac–Zoller controlled-NOT quantum gate, *Nature (London)* **422**, 408 (2003).
 - [9] W. Zwerger, Mott–Hubbard transition of cold atoms in optical lattices, *J. Opt. B* **5**, S9 (2003).
 - [10] M. Greiner, O. Mandel, T. Esslinger, T. W. Hänsch, and I. Bloch, Quantum phase transition from a superfluid to a Mott insulator in a gas of ultracold atoms, *Nature (London)* **415**, 39 (2002).
 - [11] A. J. Leggett, S. Chakravarty, A. T. Dorsey, M. P. A. Fisher, A. Garg, and W. Zwerger, Dynamics of the dissipative two-state system, *Rev. Mod. Phys.* **59**, 1 (1987).
 - [12] T. Holstein, Studies of polaron motion: Part I. The molecular-crystal model, *Ann. Phys.* **8**, 325 (1959).
 - [13] H. Fehske and S. A. Trugman, *Polarons in Advanced Materials*, edited by A. S. Alexandrov, Springer Series in Materials Science, Vol. 103 (Springer Netherlands, 2007) pp. 393–461.
 - [14] W. Chen, Y. Lu, S. Zhang, K. Zhang, G. Huang, M. Qiao, X. Su, J. Zhang, J.-N. Zhang, L. Bianchi, M. S. Kim, and K. Kim, Scalable and programmable phononic network with trapped ions, *Nat. Phys.* **19**, 877 (2023).
 - [15] H. C. J. Gan, G. Maslennikov, K.-W. Tseng, C. Nguyen, and D. Matuskevich, Hybrid quantum computing with conditional beam splitter gate in trapped ion system, *Phys. Rev. Lett.* **124**, 170502 (2020).
 - [16] W. T. Chen, J. Gan, J. N. Zhang, D. Matuskevich, and K. Kim, Quantum computation and simulation with vibrational modes of trapped ions, *Chinese Physics B* **30**, 060311 (2021).
 - [17] D. F. V. James, Quantum dynamics of cold trapped ions with application to quantum computation, *Appl. Phys. B* **66**, 181 (1998).
 - [18] S.-L. Zhu, C. Monroe, and L. M. Duan, Trapped ion quantum computation with transverse phonon modes, *Phys. Rev. Lett.* **97**, 050505 (2006).
 - [19] K. R. Brown, C. Ospelkaus, Y. Colombe, A. C. Wilson, D. Leibfried, and D. J. Wineland, Coupled quantized mechanical oscillators, *Nature (London)* **471**, 196 (2011).
 - [20] M. Harlander, R. Lechner, M. Brownnutt, R. Blatt, and W. Hansel, Trapped-ion antennae for the transmission of quantum information, *Nature (London)* **471**, 200 (2011).
 - [21] A. C. Wilson, Y. Colombe, K. R. Brown, E. Knill, D. Leibfried, and D. J. Wineland, Tunable spin–spin interactions and entanglement of ions in separate potential wells, *Nature (London)* **512**, 57 (2014).
 - [22] P.-Y. Hou, J. J. Wu, S. D. Erickson, D. C. Cole, G. Zaran-tonello, A. D. Brandt, S. Geller, A. Kwiatkowski, S. Glancy, E. Knill, A. C. Wilson, D. H. Slichter, and D. Leibfried, Coherent coupling and non-destructive measurement of trapped-ion mechanical oscillators, *Nat. Phys.* **20**, 1636 (2024).
 - [23] F. Hakeberg, P. Kiefer, M. Wittemer, U. Warring, and T. Schaetz, Interference in a prototype of a two-dimensional ion trap array quantum simulator, *Phys. Rev. Lett.* **123**, 100504 (2019).
 - [24] P. Kiefer, F. Hakeberg, M. Wittemer, A. Bermudez, D. Porras, U. Warring, and T. Schaetz, Floquet-engineered vibrational dynamics in a two-dimensional array of trapped ions, *Phys. Rev. Lett.* **123**, 213605 (2019).
 - [25] D. Porras and J. I. Cirac, Bose-Einstein condensation and strong-correlation behavior of phonons in ion traps, *Phys. Rev. Lett.* **93**, 263602 (2004).
 - [26] S. Haze, Y. Tateishi, A. Noguchi, K. Toyoda, and S. Urabe, Observation of phonon hopping in radial vibrational modes of trapped ions, *Phys. Rev. A* **85**, 031401 (2012).

- (2012).
- [27] S. Debnath, N. M. Linke, S. T. Wang, C. Figgatt, K. A. Landsman, L. M. Duan, and C. Monroe, Observation of hopping and blockade of bosons in a trapped ion spin chain, *Phys. Rev. Lett.* **120**, 073001 (2018).
- [28] M. Tamura, T. Mukaiyama, and K. Toyoda, Quantum walks of a phonon in trapped ions, *Phys. Rev. Lett.* **124**, 200501 (2020).
- [29] K. Toyoda, R. Hiji, A. Noguchi, and S. Urabe, Hong–Ou–Mandel interference of two phonons in trapped ions, *Nature (London)* **527**, 74 (2015).
- [30] P. A. Ivanov, S. S. Ivanov, N. V. Vitanov, A. Mering, M. Fleischhauer, and K. Singer, Simulation of a quantum phase transition of polaritons with trapped ions, *Phys. Rev. A* **80**, 060301(R) (2009).
- [31] K. Toyoda, Y. Matsuno, A. Noguchi, S. Haze, and S. Urabe, Experimental realization of a quantum phase transition of polaritonic excitations, *Phys. Rev. Lett.* **111**, 160501 (2013).
- [32] B. W. Li, Q. X. Mei, Y. K. Wu, M. L. Cai, Y. Wang, L. Yao, Z. C. Zhou, and L. M. Duan, Observation of non-Markovian spin dynamics in a Jaynes-Cummings-Hubbard model using a trapped-ion quantum simulator, *Phys. Rev. Lett.* **129**, 140501 (2022).
- [33] Q. X. Mei, B. W. Li, Y. K. Wu, M. L. Cai, Y. Wang, L. Yao, Z. C. Zhou, and L. M. Duan, Experimental realization of the Rabi-Hubbard model with trapped ions, *Phys. Rev. Lett.* **128**, 160504 (2022).
- [34] C. Shen, Z. Zhang, and L. M. Duan, Scalable implementation of boson sampling with trapped ions, *Phys. Rev. Lett.* **112**, 050504 (2014).
- [35] C. F. Roos, T. Monz, K. Kim, M. Riebe, H. Häffner, D. F. V. James, and R. Blatt, Nonlinear coupling of continuous variables at the single quantum level, *Phys. Rev. A* **77**, 040302 (2008).
- [36] X. R. Nie, C. F. Roos, and D. F. V. James, Theory of cross phase modulation for the vibrational modes of trapped ions, *Phys. Lett. A* **373**, 422 (2009).
- [37] K. G. Johnson, J. D. Wong-Campos, A. Restelli, K. A. Landsman, B. Neyenhuis, J. Mizrahi, and C. Monroe, Active stabilization of ion trap radiofrequency potentials, *Rev. Sci. Instrum.* **87**, 053110 (2016).
- [38] K. Cui, S. Chao, C. Sun, S. Wang, P. Zhang, Y. Wei, J. Yuan, J. Cao, H. Shu, and X. Huang, Evaluation of the systematic shifts of a $^{40}\text{Ca}^+ - ^{27}\text{Al}^+$ optical clock, *Eur. Phys. J. D* **76**, 140 (2022).
- [39] Y. Huang, P. Liu, W. Bian, H. Guan, and K. Gao, Evaluation of the systematic shifts and absolute frequency measurement of a single Ca^+ ion frequency standard, *Appl. Phys. B* **114**, 189 (2014).
- [40] F. Reif, *Fundamentals of Statistical and Thermal Physics* (Waveland Press, 2009).
- [41] Q. A. Turchette, C. J. Myatt, B. E. King, C. A. Sackett, D. Kielpinski, W. M. Itano, C. Monroe, and D. J. Wineland, Decoherence and decay of motional quantum states of a trapped atom coupled to engineered reservoirs, *Phys. Rev. A* **62**, 053807 (2000).
- [42] D. J. Wineland, C. Monroe, W. M. Itano, D. Leibfried, B. E. King, and D. M. Meekhof, Experimental issues in coherent quantum-state manipulation of trapped atomic ions, *J. Res. Natl. Inst. Stand. Technol.* **103**, 259 (1998).
- [43] X.-L. Deng, D. Porras, and J. I. Cirac, Quantum phases of interacting phonons in ion traps, *Phys. Rev. A* **77**, 033403 (2008).
- [44] C. Marquet, F. Schmidt-Kaler, and D. F. V. James, Phonon–phonon interactions due to non-linear effects in a linear ion trap, *Appl. Phys. B* **76**, 199 (2003).